RSC Advances

ROYAL SOCIETY OF CHEMISTRY

www.rsc.org/advances

Cite this: DOI: 10.1039/c0xx00000x

www.rsc.org/xxxxxx

COMMUNICATION

Enhanced visible photocatalytic activity of $BiVO_4$@β-$AgVO_3$ composite synthesized by an in-situ growth method

Yanmei Yang,[a] Yuanyuan Liu,*[a] Baibiao Huang,*[a] Rui Zhang,[b] Ying Dai,[b] Xiaoyan Qin[a] and Xiaoyang Zhang[a]

Received (in XXX, XXX) Xth XXXXXXXXX 20XX, Accepted Xth XXXXXXXXX 20XX
DOI: 10.1039/b000000x

β-$AgVO_3$ nanowires were synthesized by a simple hydrothermal process. With β-$AgVO_3$ providing V resource, $BiVO_4$@β-$AgVO_3$ composites were obtained through an in-situ growth process. $BiVO_4$@β-$AgVO_3$ composites exhibited enhanced photocatalytic properties. We discussed the possible mechanism of enhanced photocatalytic activities. The effect of content and size of $BiVO_4$ was also studied specifically.

It is well known that photocatalysis is becoming an effective technology to solve the energy shortage and environmental problems. [1-3] Besides traditional TiO_2, hundreds of photocatalysts were developed over the past decades. [4-7] However, limited absorption in visible light range and high rate of charge carriers recombination are still two basic problems existing in photocatalytic research. To overcome these limitations, lots of methods have been developed, including noble metals modification, semiconductor coupling, element doping, dye sensitization, *etc*.[2,8-10] And among these methods, composited photocatalysts exhibit excellent advantages in improving the separation efficiency of photoinduced electrons and holes due to the interface electric field. Therefore, various composites were prepared and well studied, such as Bi_2S_3/BiOCl, Bi_2S_3/$BiVO_4$ and AgI/BiOI etc.[1, 11-12]

β-$AgVO_3$ is a widely used material in cathode for lithium batteries, bacterial inactivation and H_2S sensor.[13-15] Also, it is a semiconductor with excellent optical absorption in visible light region. However, its studies in photocatalytic property are very limited. Only several reports are focused on the degradation of organic pollutants over β-$AgVO_3$,[16-17] compared to other famous Ag-based materials such as AgCl, Ag_3PO_4[18-19]. The main reason can be attributed to the rapid recombination of photoinduced charge carriers. Therefore, researches on enhancing the separation of charge carriers for β-$AgVO_3$ are of great importance and value to break through its limited application in photocatalysis.

$BiVO_4$ is a good choice to form heterojunction structure with β-$AgVO_3$. The matched energy band levels between the two materials can enhance the separation of photoinduced electrons and holes. Moreover, as β-$AgVO_3$ can be used as V resource, in-situ growth of $BiVO_4$ at β-$AgVO_3$ can be realized. And via in-situ growth, $BiVO_4$ nanoparticles can be distributed and fixed on the surface of β-$AgVO_3$, which would suppress the easy aggregation of $BiVO_4$. In addition, the closely touched interfaces between $BiVO_4$ and β-$AgVO_3$ are favorable for charge carries separation. $BiVO_4$ materials are chemical stable, low cost and non-toxicity, and are extensively applied as an environmentally friendly photocatalyst to produce O_2 from water and decompose organic pollutants.[20-21] However, its photocatalytic activity is still limited by the low quantum yield, even though $BiVO_4$ possesses good absorption in visible light range. Thus, several methods are developed to improve its photocatalytic activity. And coupling with other semiconductors was proved to be an effective way and various $BiVO_4$ based composites were developed, such as Bi_2S_3/$BiVO_4$, $BiVO_4$/WO_3.[11, 22] However, to the best of our knowledge, no report was found on $BiVO_4$@β-$AgVO_3$ composite and its photocatalytic activity.

Herein, we prepared $BiVO_4$@β-$AgVO_3$ composite by an in-situ growth process. β-$AgVO_3$ can not only provide V resource but also immobilize the generated $BiVO_4$ nanoparticles.The composite displayed enhanced photocatalytic activity when compared with single $BiVO_4$ or β-$AgVO_3$ under visible light irradiation. We discussed the mechanism of enhanced properties from aspects of morphology, optical absorption property, BET surface area and energy band levels between the two materials. Morphology and matched energy band levels are the major factors for improved photocatalytic activity of $BiVO_4$@β-$AgVO_3$ composite.

Fig. 1a shows the XRD patterns of as-prepared β-$AgVO_3$, $BiVO_4$, and $BiVO_4$@β-$AgVO_3$ composites. The diffraction peak positions of the prepared β-$AgVO_3$ are identical to the standard cards (JCPDS 29-1154), which suggests that the prepared β-$AgVO_3$ has a monoclinic structure (Fig. S1). However, the peak intensity are different, and the peaks for (5 0 1) facets in the prepared β-$AgVO_3$ is much stronger, while that for (-2 1 1) and (-4 1 1) facets are much weaker. The results indicate the preferential orientation of β-$AgVO_3$. $BiVO_4$ shows a monoclinic scheelite structure (JCPDS 14-0688) which displays the best photocatalytic activity among the three tetragonal, orthorhombic, and monoclinic phases (Fig. S2).[23] For the composite, $BiVO_4$@β-$AgVO_3$-5% has very weak diffraction intensity of $BiVO_4$ because of the low content. And with increasing of $BiVO_4$ content, its diffraction intensity becomes stronger gradually. Meanwhile, the peaks of β-$AgVO_3$ do not shift, indicating that the introduction of $BiVO_4$ does not change the crystal structure of β-$AgVO_3$. In Fig. 1b, the intensity ratio of typical peak of (-1 2 1) for $BiVO_4$ to that of (5 0 1) for β-$AgVO_3$ is given. It clearly shows that with increasing $BiVO_4$ content from 5% to 20%, this ratio increases steadily, which further proves the increasing amounts of $BiVO_4$ in $BiVO_4$@β-$AgVO_3$ composites.

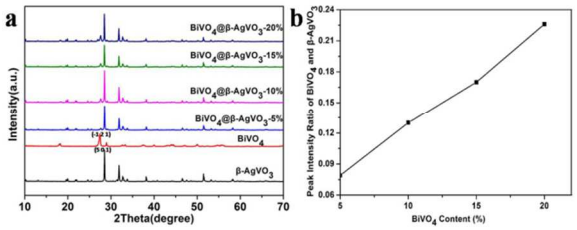

Fig. 1 XRD patterns of as-prepared products (a) and the intensity ratio of typical peaks of (-1 2 1) for $BiVO_4$ to (5 0 1) for β-$AgVO_3$.

The SEM images of pure β-$AgVO_3$ and $BiVO_4$@β-$AgVO_3$ composites with different contents of $BiVO_4$ are presented in Fig. 2. From Fig. 2a we can see that β-$AgVO_3$ shows nanowire morphology with a size of about 200nm in width and more than 10 μm in length, and the surface is very smooth. In addition, the lattice fringes with interplanar spacing of 0.775 nm corresponding to the (-1 0 1) plane are measured, while the growth direction is perpendicular to plane (-1 0 1). That is to say the preferential orientation of β-$AgVO_3$ nanowires are along (0 1 0) direction which is consistent with the previous research.[14] For the composite (Fig. 2b-e), when $BiVO_4$ is 5%, several $BiVO_4$ nanoparticles with the size of about 80 nm are dispersed on the surface of β-$AgVO_3$ by the in-situ growth process (Fig.2b). With increasing of $BiVO_4$ content, more $BiVO_4$ nanoparticles are formed and the size has a small tendency to be larger (Table 1), which is in agreement with the enhanced intensity of XRD peaks. In Fig. 2e, when $BiVO_4$ content reaches to 20%, β-$AgVO_3$ nanowires are covered with $BiVO_4$ nanoparticles with the size of about 175 nm. The $BiVO_4$ prepared for comparison shows irregular board-like morphology with a size of 1-2 μm (Fig. S3). Therefore, the in-situ growth method is favorable for the formation of nanoparticles and prevents the aggregation of $BiVO_4$.

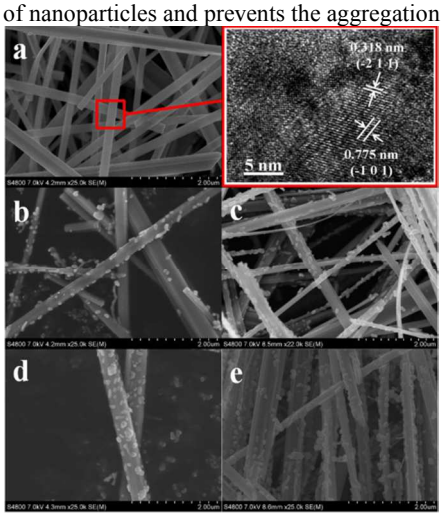

Fig. 2 SEM and HR-TEM images of β-$AgVO_3$ (a), SEM images of $BiVO_4$@β-$AgVO_3$-5% (b), $BiVO_4$@β-$AgVO_3$-10% (c), $BiVO_4$@β-$AgVO_3$-15% (d), $BiVO_4$@β-$AgVO_3$-20% (e).

To illustrate the optical absorption properties of $BiVO_4$@β-$AgVO_3$ composites, DRS spectra were measured, as can be seen in Fig. 3a. For comparison, the spectra of pure β-$AgVO_3$ and $BiVO_4$ are also given. It shows that both β-$AgVO_3$ and $BiVO_4$ have good optical absorption in visible light, with a clear absorption edge at around 551 nm and 506 nm, respectively. The composite has a small difference with a little shift of absorption edge from 551 nm to 506 nm. To obtain the band gaps of β-$AgVO_3$ and $BiVO_4$, we cited the formular: [12] $\alpha h\upsilon = A(h\upsilon - E_g)^{n/2}$, where α is the absorption coefficient, $h\upsilon$ is the discrete photon energy, A is a constant, and E_g is the band gap. The value of n depends on whether the transition is direct (n = 1) or indirect (n = 4) in a semiconductor. β-$AgVO_3$ and $BiVO_4$ are direct transition semiconductor, thus n is 1.[16,22] The curve of $(\alpha h\upsilon)^2$ versus $h\upsilon$ is given in Fig. 3b. When $(\alpha h\upsilon)^2$ is set as 0, we can get the band gap E_g of β-$AgVO_3$ and $BiVO_4$ to be 2.25 eV and 2.45 eV, respectively.

Furthermore, the position of CB minimum and VB maximum are determined. For a semiconductor at the point of zero charge, its VB edge can be calculated by the empirical equation $E_{VB} = \chi - E^e + \frac{1}{2}E_g$, in which E_{VB} is the valence band-edge potential, χ is the electronegativity of the semiconductor, expressed as the geometric mean of the absolute electronegativity of the constituent atoms, E^e is the energy of free electrons on hydrogen scale with the value of about 4.5 eV, E_g is the bandgap energy of a semiconductor, and E_{CB} can be obtained by the equation $E_{CB} = E_{VB} - E_g$.[24] For β-$AgVO_3$, χ is about 5.88 eV and E_g is 2.25 eV, so its top of VB is calculated to be 2.50 eV. Accordingly, its bottom of CB is calculated to be 0.25 eV. In the same way, χ value of $BiVO_4$ is 6.07 eV, its E_{VB} and E_{CB} are 2.8 eV and 0.35 eV, respectively.

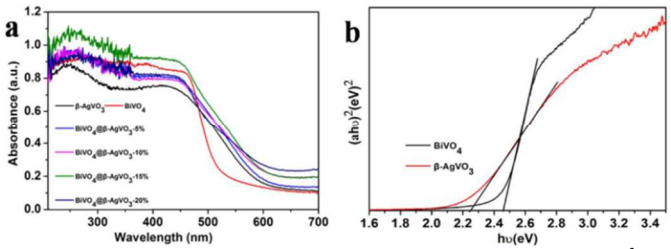

Fig. 3 DRS spectra of as-prepared products (a) and the plots of $(\alpha h\upsilon)^2$ versus $h\upsilon$ of β-$AgVO_3$ and $BiVO_4$ (b).

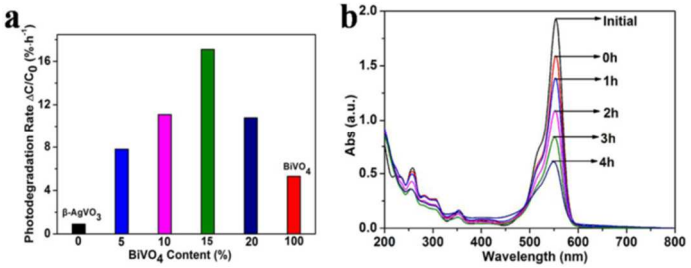

Fig. 4 The average photodegradation rates of as-prepared products (a) and the temporal evolution of the absorption spectra of RhB solution by β-$BiVO_4$@β-$AgVO_3$-15% (b).

The photocatalytic activities of as-prepared samples were evaluated by photodegradation of RhB under visible light irradiation at room temperature. Fig. 4a displays the average degradation rates of $BiVO_4$@β-$AgVO_3$ composites (0, 5%, 10%, 15%, 20%) under visible light irradiation for 4h. For comparison, the photocatalytic activities of pure β-$AgVO_3$ and $BiVO_4$ were also measured under the same condition. Obviously, β-$AgVO_3$@$BiVO_4$ composites can degrade RhB more effectively than pure β-$AgVO_3$ and $BiVO_4$ and the photocatalytic activities of composites are affected dramatically by the content of $BiVO_4$. The best activity comes from $BiVO_4$@β-$AgVO_3$-15% with 17.1% · h^{-1}, while the rates are 0.9% · h^{-1} and 7.8% · h^{-1} over pure β-$AgVO_3$ and $BiVO_4$@β-$AgVO_3$-5%, respectively. In addition, the $BiVO_4$@β-$AgVO_3$-10% and $BiVO_4$@β-$AgVO_3$-20% show nearly the same degradation rates, 11.1% · h^{-1} and 10.8% · h^{-1}. As

Table 1 BET values and average photodegradation rate of RhB for β-$AgVO_3$, $BiVO_4$, and β-$AgVO_3$@$BiVO_4$ composites.

Sample code	a	b	c	d	e	f
$BiVO_4$ molar ratio(%)	0	100	5	10	15	20
Average size of $BiVO_4$(nm)	-	-	80	100	140	175
BET($m^2 \cdot g^{-1}$)	2.8042	1.2115	4.6333	6.2214	3.8801	7.1321
Average photodegradation rate of RhB $\Delta C/C_0$ (h^{-1})	0.9%	5.3%	7.8%	11.1%	17.1%	10.8%

a result, it can be concluded that the optimal $BiVO_4$ content is 15% for the $BiVO_4$@β-$AgVO_3$ compiste. Fig. 4b shows the temporal evolution of the absorption spectra of RhB solution with $BiVO_4$@β-$AgVO_3$-15% composite. We can see the absorption at 554nm decreases gradually under visible light irradiation, which indicates the effective degradation of RhB. The TOC (total organic carbon) before and after photocatalysis by $BiVO_4$@β-$AgVO_3$-15% was evaluated with the value of 8.793 $mg \cdot L^{-1}$ and 5.779 $mg \cdot L^{-1}$, respectively. We can confirm after 4h under visible light irradiation, TOC decreased by 34.3%. Thus, we concluded that it is possible for Rhodamine B to be converted to CO_2 eventually.

To explain the photocatalytic mechanism of different photocatalytic activities, the possible factors including surface areas, optical absorption properties, morphologies and energy band structure of composite are discussed below. The BET specific surface areas and average photodegradation rate of pure β-$AgVO_3$, $BiVO_4$, and $BiVO_4$@β-$AgVO_3$ composites are presented in Table 1. It shows that the specific BET surface areas of β-$AgVO_3$ and $BiVO_4$ are very small and the introduction of different $BiVO_4$ contents does not have large effect. In addition, the change of BET surface areas does not show the same tendency with that of average photodegradation rate. Therefore, it can be concluded that the BET surface areas make little contribution to the enhanced and various photocatalytic activities of $BiVO_4$@β-$AgVO_3$ composites. In terms of the optical absorption properties, from the previous analysis it can be seen both of β-$AgVO_3$ and $BiVO_4$ have good optical absorption in visible light region. And the coupling between them does not make large difference, only leading to a little shift of absorption edge. So it is not the major factor in the photodegradation process. The main factors that affect the activities of as-prepared products lie in the energy band structure of β-$AgVO_3$ and $BiVO_4$ and the varied amounts and morphologies with increasing of $BiVO_4$ content, which will be illustrated specifically in the following.

Fig. 5 illustrates the band energy levels of β-$AgVO_3$ and $BiVO_4$ and the possible charge separation process, According to above calculation. Under visible light irradiation, both of β-$AgVO_3$ and $BiVO_4$ can be excited and generate electrons and holes. As the CB of β-$AgVO_3$ (0.25 eV) is more negative than that of $BiVO_4$ (0.35 eV), while the VB of $BiVO_4$ (2.80 eV) is more positive than that of β-$AgVO_3$ (2.50 eV), the photoinduced electrons on the CB of β-$AgVO_3$ can transfer to the CB of $BiVO_4$ and the holes will pass from the VB of $BiVO_4$ to the VB of β-$AgVO_3$. In this process, the simultaneously occurred transfer of electrons and holes decrease charge carriers' recombination possibility, increase their quantum yield and lifetime. So, electrons on CB of $BiVO_4$ can be consumed by reducing absorbed O_2 molecules to OH^-, considering the more negative potential (0.35 eV) compared to the reduction potential of O_2/OH^- (0.401 eV), while the holes can be consumed by two pathways. Ⅰ.Can be used for the direct degradation of RhB.[25] Ⅱ. Oxidize the surface OH^- to ·OH due to the more positive potential than the standard oxidation potential of OH^-/·OH (1.99eV),[26] which plays an important role in oxidative degradation of RhB.[27] As a result, charge carriers can be separated effectively and enhance the photocatalytic activities of $BiVO_4$@β-$AgVO_3$ composites.

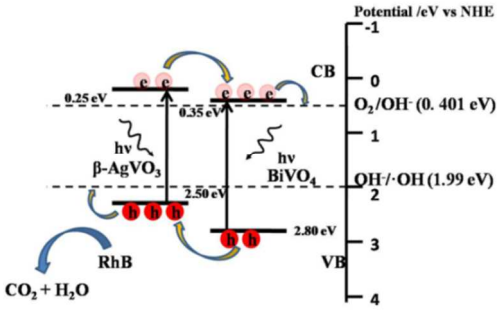

Fig. 5 Schematic diagram for energy band of β-$AgVO_3$ and $BiVO_4$ and the possible charge separation mechanism

With increasing content of $BiVO_4$, the activities of composites increase firstly and then decrease, the reason of which is attributed to the different contents and morphologies of $BiVO_4$. Firstly, with increase of $BiVO_4$ content (5%-15%), more $BiVO_4$ nanoparticles (about 100-150nm) are formed on the surface of β-$AgVO_3$ nanowires, effectively enhancing the charge carriers separation for the degradation reaction. Thus, the photocatalytic activity is obviously improved. However, when the $BiVO_4$ content increases further, the composite photocatalytic activity declines, implying the high content of $BiVO_4$ is unfavorable for the photodegradation. The reason is that the excessive $BiVO_4$ nanoparticles with larger size (150-200nm) may act as mediators for recombination of photoinduced electrons and holes. Therefore, considering the synergistic effect of content and size of $BiVO_4$ nanoparticles, there is an optimal ratio between β-$AgVO_3$ and $BiVO_4$, and the $BiVO_4$@β-$AgVO_3$-15% exhibits the best photocatalytic activity.

In summary, we have prepared pure β-$AgVO_3$ nanowires using a simple hydrothermal method. Furthermore, $BiVO_4$@β-$AgVO_3$ composites were synthesized via in-situ growth of $BiVO_4$, and β-$AgVO_3$ nanowires acted as not only V resources, but also effective framework to immobilize $BiVO_4$ nanoparticles. The $BiVO_4$@β-$AgVO_3$ composites showed better photocatalytic performance than pure β-$AgVO_3$ and $BiVO_4$ in degradation of RhB dye under visible light. The reason is attributed to the matched energy band structure formed in the heterojunction that can effectively enhance the separation of photoinduced electrons and holes.

This work is financially supported by a research Grant from the National Basic Research Program of China (the 973 Program; No. 2013CB632401), the National Natural Science Foundation of China (No. 21333006, 11374190 and 51021062).

Notes and references

[a] *State key lab of crystal materials, Shandong university, Jinan, China, 250100. Email: bbhuang@sdu.edu.cn（Baibiao Huang）, yyliu@sdu.edu.cn （Yuanyuan Liu）*

[b] *School of physics, Shandong university, Jinan, China, 250100.*

† Electronic Supplementary Information (ESI) available: Experimental details, Figure S1-S3. See DOI: 10.1039/b000000x/

1 H. F. Cheng, B. B. Huang, X. Y. Qin, X. Y. Zhang, Y. Dai *Chem. Commun.*, 2012, **48**, 97.
2 P. Wang, J. Wang, T. S. Ming, X. F. Wang, H. G. Yu, J. G. Yu, Y. G. Wang, M. Lei, *ACS Appl. Mat. Interfaces.*, 2013, **5**, 2924.
3 W. L. Yang, L. Zhang, Y. Hu, Y. J. Zhong, H. B. Wu, X. W. D. Lou, *Angew. Chem. Int. Ed.*, 2012, **51**, 11501.
4 M. Ni, M. K. Leung, D. Y. Leung, K. Sumathy, *Renewable Sustainable Energy Rev.*, 2007, **11**, 401.
5 S. Chakrabarti, B. K. Dutta, *J. Hazard. Mater.*, 2004, **112**, 269.
6 Y. Park, K. J. McDonald, K.-S. Choi, *Chem. Soc. Rev.*, 2013, **42**, 2321.
7 S. N. Habisreutinger, L. Schmidt‐Mende, J. K. Stolarczyk, *Angew. Chem. Int. Ed*., 2013, **52**, 7372.
8 L. Q. Jing, D. J. Wang, B. Q. Wang, S. D. Li, B. F. Xin, H. G. Fu, J. Z. Sun, *J. Mol. Catal. A: Chem.*, 2006, **244**, 193.
9 G. Ghadimkhani, N. R. de Tacconi, W. Chanmanee, C. Janaky, K. Rajeshwar, *Chem. Commun*., 2013, **49**, 1297.
10 S. Usai, S. Obregón, A.I. Becerro, G. Colón, *J. Phys. Chem. C*, 2013, **117**, 24479.
11 D.-K. Ma, M.-L. Guan, S.-S. Liu, Y.-Q. Zhang, C.-W. Zhang, Y.-X. He, S.-M. Huang, *Dalton Trans.*, 2012, **41**, 5581.
12 H. F. Cheng, B. B. Huang, Y. Dai, X. Y. Qin, X. Y. Zhang, *Langmuir.*, 2010, **26**, 6618.
13 F. Y. Cheng, J. Chen, *J. Mater. Chem.*, 2011, **21**, 9841.
14 J. Ren, W. Z. Wang, M. Shang, S. M. Sun, L. Zhang, J. Chang, *J. Hazard. Mater.*, 2010, **183**, 950.
15 L. Q. Mai, L. Xu, Q. Gao, C. H. Han, B. Hu, Y. Q. Pi, *Nano Lett.*, 2010, **10**, 2604.
16 J. Xu, C. G. Hu, Y. Xi, B. Y. Wan, C. L. Zhang, Y. Zhang, *Solid State Sci.*, 2012, **14**, 535.
17 G.-T. Pan, M.-H. Lai, R.-C. Juang, T.-W. Chung, T.C.-K. Yang, *Ind. Eng. Chem. Res.*, 2011, **50**, 2807.
18 P. Wang, B. B. Huang, X. Y. Zhang, X. Y. Qin, Y. Dai, Z. Y. Wang, Z. Z. Lou, *ChemCatChem.*, 2011, **3**, 360.
19 Y. P. Bi, S. X. Ouyang, N. Umezawa, J. Y. Cao, J. H. Ye, *J. Am. Chem. Soc.*, 2011, **133**, 6490.
20 G. M. Wang, Y. C. Ling, X. H. Lu, F. Qian, Y. X. Tong, J. Z. Zhang, V. Lordi, C. Rocha Leao, Y. Li, *J. Phys. Chem. C*, 2013, **117**, 10957.
21 D. G. Wang, H. F. Jiang, X. Zong, Q. Xu, Y. Ma, G. L. Li, C. Li, *Chem. Eur. J.* , 2011, **17**, 1275.
22 S. J. Hong, S. Lee, J. S. Jang, J. S. Lee, *Energy Environ. Sci.*, 2011, **4**, 1781.
23 J. Q. Yu, A. Kudo, *Adv. Funct. Mater.*, 2006, **16**, 2163.
24 Y. Xu, M.A. Schoonen, *Am. Mineral.*, 2000, **85**, 543.
25 X. K. Li, J. H. Ye, *J. Phys. Chem. C*, 2007, **111**, 13109.
26 H. B. Fu, C. S. Pan, W. Q. Yao, Y. F. Zhu, *J. Phys. Chem. B*, 2005, **10**9, 22432.
27 H. M. Sung-Suh, J.R. Choi, H.J. Hah, S.M. Koo, Y.C. Bae, *J. Photochem. Photobiol., A*, 2004, **163**, 37.

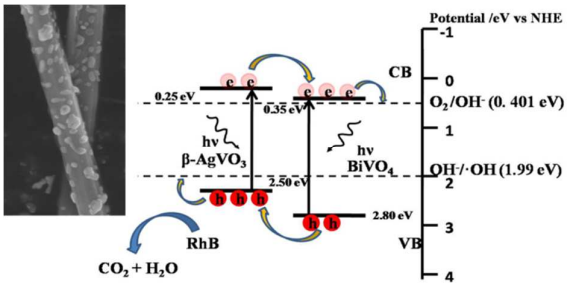

Novel $BiVO_4$@β-$AgVO_3$ composite synthesized by an in-situ growth method on surface of β-$AgVO_3$ nanowires exhibited enhanced visible photocatalytic activity.

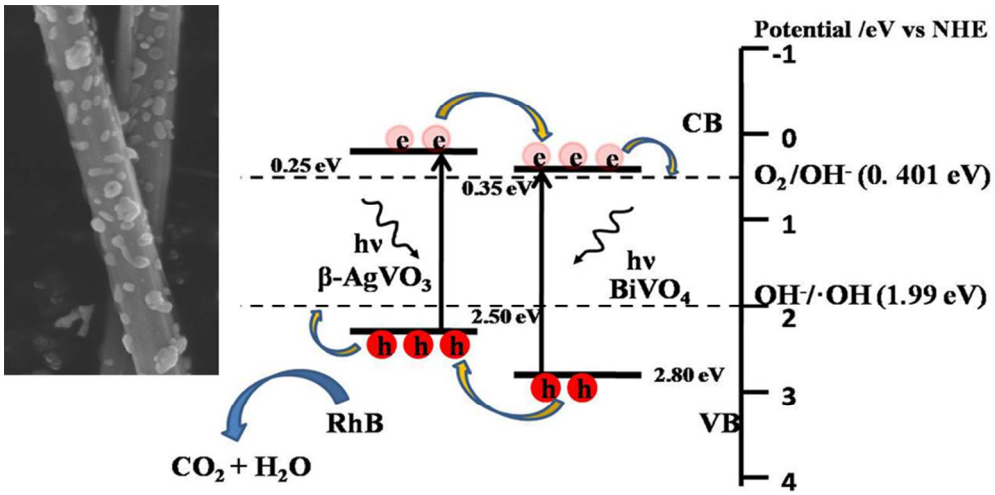

80x39mm (300 x 300 DPI)